

Deep Pyramidal Residual Networks

Dongyoon Han*
EE, KAIST

dyhan@kaist.ac.kr

Jiwhan Kim*
EE, KAIST

jhkim89@kaist.ac.kr

Junmo Kim
EE, KAIST

junmo.kim@kaist.ac.kr

Abstract

Deep convolutional neural networks (DCNNs) have shown remarkable performance in image classification tasks in recent years. Generally, deep neural network architectures are stacks consisting of a large number of convolution layers, and they perform downsampling along the spatial dimension via pooling to reduce memory usage. At the same time, the feature map dimension (i.e., the number of channels) is sharply increased at downsampling locations, which is essential to ensure effective performance because it increases the capability of high-level attributes. Moreover, this also applies to residual networks and is very closely related to their performance. In this research, instead of using downsampling to achieve a sharp increase at each residual unit, we gradually increase the feature map dimension at all the units to involve as many locations as possible. This is discussed in depth together with our new insights as it has proven to be an effective design to improve the generalization ability. Furthermore, we propose a novel residual unit capable of further improving the classification accuracy with our new network architecture. Experiments on benchmark CIFAR datasets have shown that our network architecture has a superior generalization ability compared to the original residual networks.

Code is available at <https://github.com/jhkim89/PyramidNet>

1. Introduction

The emergence of deep convolutional neural networks (DCNNs) has greatly contributed to performing extensive tasks [13, 23, 2, 3, 19] in computer vision with significantly improved performance. Since the proposal of LeNet [16] as the starting point of a deep neural network architecture for computer vision tasks, the advanced architecture AlexNet [13] was spotlighted to win the 2012 ImageNet competition [22] by a large margin over traditional methods. Subsequently, ZF-net [34], VGG [25], GoogleNet [31], Residual Networks [6, 8], and Inception Residual Net-

works [30] were successively proposed to demonstrate the advance in network architectures. In particular, Residual Networks (ResNets) [6, 8] leverage the concept of shortcut connections [29] inside a proposed residual unit for residual learning to make it possible to train much deeper network architectures. Deeper network architectures are known for their superior performance and these network architectures commonly have deeply stacked convolutional filters with nonlinearity [25, 31].

In respect of the feature map dimension, the conventional way of stacking several convolutional filters is to increase the dimension while decreasing the size of feature maps by increasing the strides of the filters or poolings. This is widely adopted because controlling the size of feature maps is effective for reducing the classification tasks to condense the information of sources with increased dimension (i.e., increased filters). Architectures such as those of VGG [25] and GoogleNet [31] utilize this way of increasing the feature map dimension to construct their network architecture, and the most successful deep neural network, ResNets [6, 8], which was introduced by He *et al.* [6], also follows this approach for filter stacking.

According to the research of Veit *et al.* [32], ResNets are considered to operate as ensembles of relatively shallow networks. These researchers showed that the deletion of an individual residual unit from ResNets, i.e., such that only a shortcut connection remains, does not significantly affect the overall performance, proving that deleting a residual unit is equivalent to deleting some shallow networks in the ensemble networks. Contrary to this, deleting a single layer in plain network architectures such as a VGG-network [25] damages the network to incur severe additional errors.

However, in the case of ResNets, they found that deleting the building block in a residual unit with downsampling still affects the classification error by a large margin. This phenomenon mainly occurs because the feature map dimension is suddenly increased at the units subjected to downsampling. This approach is commonly used [6, 25] to prevent the loss of information incurred by downsampling, and to obtain additional high-level attributes because the feature map is downsampled by increasing the number of fea-

*These two authors contributed equally.

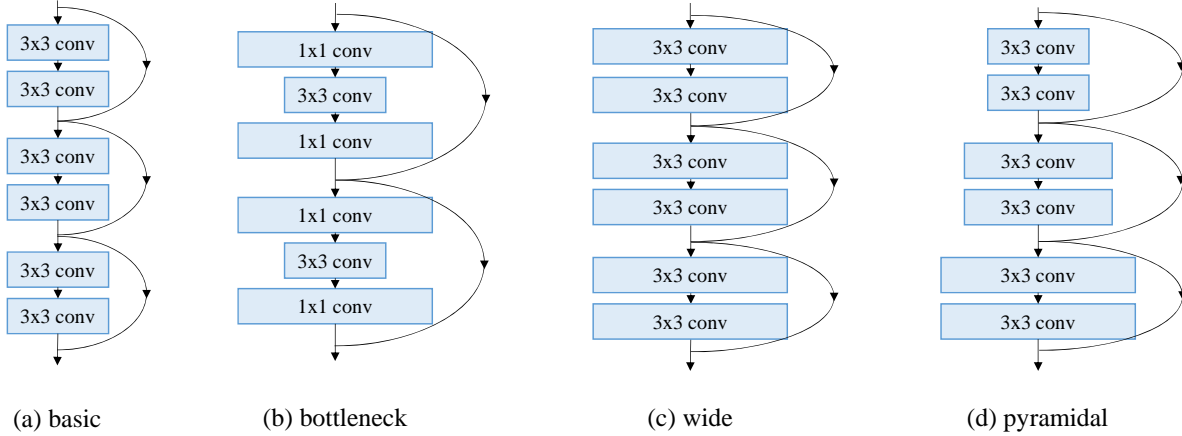


Figure 1. Schematic illustration of (a) basic residual units [6], (b) bottlenecks [6], (c) wide residual units [33], and (d) our pyramidal residual units.

ture maps. Therefore, as shown in [32], when the building blocks in residual units subjected to downsampling are deleted, the remaining shortcut connection seems to have difficulty in adjusting to the role of the deleted unit. This enlarges the feature dimension, and results in performance loss.

Inspired by their hypothesis, we suggest a way to remedy this phenomenon, by increasing the feature map dimensions at all layers to distribute the burden concentrated at locations of residual units affected by downsampling such that it is equally distributed across all units. In our paper, we refer to this network architecture as a deep “pyramidal” network and a “pyramidal” residual network with a residual-type network architecture. This reflects the fact that the shape of the network architecture can be compared to that of an ancient pyramid. That is, the number of channels gradually increases as a function of the depth at which layers occur, which is similar to a pyramid structure of which the shape gradually widens from the top downwards. This structure is illustrated in comparison to other network architectures in Figure 1. The key contributions are summarized as follows:

- A deep pyramidal residual network (PyramidNet) is introduced. The key idea is to concentrate on the feature map dimension by increasing it gradually instead of by increasing it sharply at each residual unit with downsampling.
- A novel residual unit is proposed as well, which can further improve the performance of ResNet-based architectures, compared with state-of-the-art network architectures.
- We also show that our network architecture can take advantages of the both plain and residual networks by using zero-padded shortcut connections when in-

creasing the filter dimension, and this was found to improve the performance and reduce the computational complexity compared with the projection shortcut and other overly wide networks [33].

The remainder of this paper is organized as follows. Section 2 presents our PyramidNets and introduces a novel residual unit that can further improve ResNet. Section 3 studies closely our PyramidNets with several items. Section 4 presents the experimental results and comparisons with several state-of-the-art deep network architectures. Section 5 concludes our paper with future works.

2. Network Architecture

In this section, we introduce the network architecture of our PyramidNets. The major difference compared with other network architectures is that the dimension of channels gradually increases, instead of maintaining the dimension until a downsampling residual unit appears. A schematic illustration is appears in Figure 1 (d) to facilitate understanding of our network architecture.

2.1. Feature Map Dimension Increasing

Most deep CNN architectures [6, 8, 13, 25, 31, 34] utilize an approach whereby feature map dimensions are increased by a large margin when the size of the feature map decreases, and feature map dimensions are not increased until they encounter a residual unit with downsampling. In the case of the original ResNet for CIFAR datasets [12], the number of feature dimensions $D_{n,k}$ of the k -th residual unit of the n -th group can be described as below:

$$D_{n,k} = \begin{cases} 16, & \text{if } (n, k) = (1, 1) \\ 16 \cdot 2^{n-2}, & \text{otherwise} \end{cases} \quad (1)$$

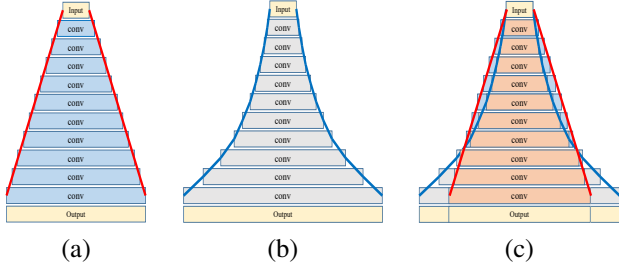


Figure 2. Visual illustrations of (a) additive PyramidNet, (b) multiplicative PyramidNet, and (c) a comparison of (a) and (b).

in which $n \in \{1, 2, 3, 4\}$ denotes the number of groups that have an equal feature map size and contain N residual units except for $n = 1$. In the case of $n = 1$, it has only one convolutional layer that converts an RGB image into multiple feature maps. After N residual units have passed, the feature size is downsampled by a half and the number of dimensions is doubled. In our work, we define the approach of increasing the feature map dimension as below:

$$D_{n,k} = \begin{cases} 16 + (n-1)\delta, & \text{if } n \geq 2, k = 1 \\ D_{n,k-1} + \lfloor \alpha k/N + 0.5 \rfloor, & \text{if } n \geq 2, k > 1 \end{cases} \quad (2)$$

such that the dimension is increased by a step factor of $\lfloor \alpha k/N \rfloor$, and the output dimension of the final unit of each group becomes $16 + \alpha(n-1)$. The details of our network architecture are presented in Table 1. Note that δ in the table is set by α as stated in the table, from which eq.(2) is derived.

The above equations are based on an addition-based widening step factor α for increasing dimensions. However, of course, multiplication-based widening (i.e., the process of multiplying by a factor to increase the channel dimension geometrically) presents another possibility for creating a pyramid-like structure. Then, eq.(2) can be transformed as below:

$$D_{n,k} = D_{n,k-1} \cdot \alpha^{\frac{1}{N}}, \quad (n \geq 2). \quad (3)$$

The main difference between additive and multiplicative PyramidNets is that the feature dimension of an additive network gradually increases as a result of linear decay, whereas the dimension of a multiplicative network increases geometrically. That is, the dimension slowly increases in the upper layers that are close to the input and sharply increases in the lower layers. This process is similar to that of the original deep network architectures such as VGG [25] and ResNet [6]. The visual illustrations of the additive and multiplicative PyramidNets are shown in Figure 2. In this paper, we compare the performance of both of these approaches to increasing the dimension by comparing

Group	Output size	Building Block
conv1	32×32	$[3 \times 3, 16]$
conv2_k	32×32	$\begin{bmatrix} 3 \times 3, \lfloor \alpha k/N + 16 \rfloor \\ 3 \times 3, \lfloor \alpha k/N + 16 \rfloor \end{bmatrix} \times N$
conv3_k	16×16	$\begin{bmatrix} 3 \times 3, \lfloor \alpha k/N + 16 + \delta \rfloor \\ 3 \times 3, \lfloor \alpha k/N + 16 + \delta \rfloor \end{bmatrix} \times N$
conv4_k	8×8	$\begin{bmatrix} 3 \times 3, \lfloor \alpha k/N + 16 + 2\delta \rfloor \\ 3 \times 3, \lfloor \alpha k/N + 16 + 2\delta \rfloor \end{bmatrix} \times N$
Avg pool	1×1	8×8

Table 1. Structure of our PyramidNet for benchmarking with CIFAR datasets. α denotes the widening factor, δ denotes the offset factor, and N signifies the number of blocks in a group. Down-sampling is performed at conv3_1 and conv4_1 with a stride of 2. For our PyramidNets, we set δ as the final dimension of the previous channel that is α . Thus, the dimension of the output channel of the final block for each group is $\{16, 16 + \alpha, 16 + 2\alpha, 16 + 3\alpha\}$, respectively.

an additive PyramidNet (eq. (3)) and a multiplicative PyramidNet (eq. (2)) in section 4.

2.2. Building Block

The building block (i.e., the convolutional filter stacks with ReLUs and BN layers) in a residual unit is the core of ResNet-based architectures. It is obvious that in order to maximize the capability of the network architecture, designing a good building block is essential. As we can see in Figure 6, the layers can be stacked in various ways to construct a single building block. We found the architecture shown in Figure 6 (d) to be the most promising building block, and therefore we included this structure in our building block for PyramidNets. The discussion of this matter is continued in the following section.

In terms of shortcut connections, many researchers either use those based on identity-mapping, or those employing convolution-based projection. However, as the channel dimension of our network is increased at every unit, we can only consider two options: identity with zero-padding shortcuts, and projection shortcuts conducted by 1×1 convolutions. Yet, as mentioned in the work of He *et al.* [8], the 1×1 convolutional shortcut produces a poor result when there are too many residual units, i.e., this shortcut is unsuitable for very deep network architectures. Therefore, we selected an identity with zero-padding for all shortcut connections. Further discussions about the zero-padded connection are provided in the next section.

3. Discussions with PyramidNet

In this section, we present an in-depth study of the architecture of our PyramidNet together with the proposed novel residual units. The experiments we include here support the study and confirm that insights obtained from our network

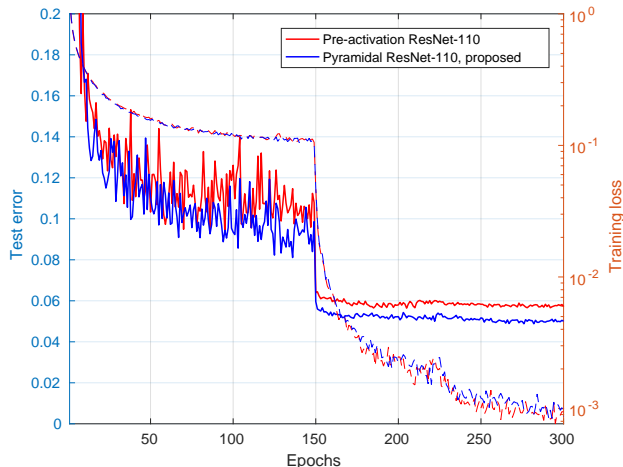


Figure 3. Performance comparison on CIFAR datasets between the pre-activation ResNet [8] and our PyramidNet. Dashed and solid lines denote the training loss and test error, respectively.

architecture can further improve the performance of existing ResNet-based architectures.

3.1. Effect of PyramidNet

According to the work of Veit *et al.* [32], ResNets can be described as ensembles of relatively shallow networks, showing that deleting an individual building block in a residual unit of ResNets affects minor classification loss, whereas removing layers from plain networks such as VGG [25] severely reduces the classification rate. However, in original and pre-activation ResNets [6, 8], another noteworthy aspect is that deleting the blocks with downsampling still degrades the performance by a large margin [32]. As mentioned before, this problem is mainly due to these units doubling the feature map dimension, and they play a very important role in the overall network.

However, some “intrinsic” ensembles encompassing these residual units occupy more important roles in the overall performance than other ensembles do, and therefore this may reduce the generalization ability by combining other intrinsic ensembles. As proof, the stochastic depth [10] can further improve the network performance, because it enables each residual unit to be trained independently, such that the ensemble effect of shallow networks is strengthened. At the same time, a model trained with stochastic depth does not affect the classification performance when an individual block is deleted, including the blocks in residual units subjected to downsampling [10]. Therefore, to maximize the ensemble effect, we attempt to gradually increase the feature map dimension instead of doubling it at one of the residual units, to evenly distribute the burden of increasing the feature maps.

The training and test curves of our network are compared

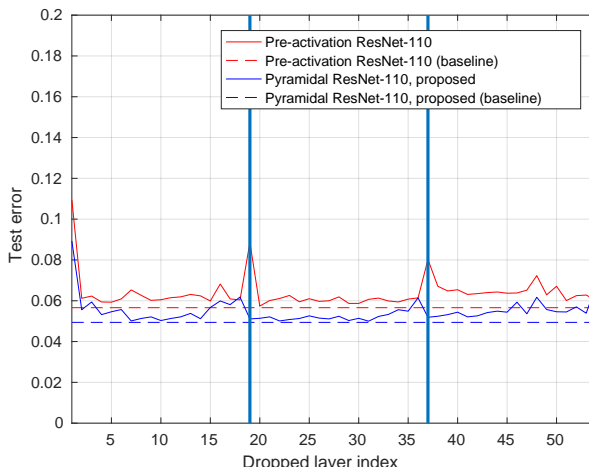


Figure 4. Test error curves to study the extent to which units contribute to the performance in different network architectures. Deletion of individual building blocks in two network architectures (our PyramidNet and the pre-activation ResNet [8]) enables us to determine which residual units contribute most to their performance. The dashed and solid lines denote the test error without deleting blocks and when an individual block is deleted, respectively. Bold vertical lines denote the location of residual units with downsampling.

with those of the pre-activation ResNet [8] in Figure 3. We use the standard pre-activation ResNet with 110 layers for comparison. For our pyramidal networks, we use a depth of 110 with a widening factor of $\alpha = 16$, which has the same number of parameters (1.7M) as the pre-activation ResNet to allow for fair comparison. Our results indicated that our network has superior test accuracy, thereby confirming its greater ability to generalize than original deep networks.

We verified the ensemble effect of our pyramidal networks by evaluating the performance of our network after deleting individual blocks, similar to the experiment of Veit *et al.* [32]. The results are shown in Figure 4. As mentioned by Veit *et al.* [32], removing individual blocks only affects a slight performance loss, compared with a plain network such as the VGG [25] model. However, in the case of the original ResNet, removing the blocks subjected to downsampling tends to affect the accuracy by a relatively large margin, whereas this does not occur with our pyramidal networks. Furthermore, the mean average error difference between the baseline result and the result obtained when individual blocks are deleted from both the original ResNet and our PyramidNet is 0.72% and 0.54%, respectively. This result shows that the ensemble effect of our network becomes stronger than the original ResNet, such that the generalization ability is improved.

3.2. Zero-padded Shortcut Connection

Original ResNets [6] were based on three suggested types of shortcut connections between the input and output of each residual unit: 1) identity-mapping shortcut, and identity-mapping with zero-padded shortcut at residual units with downsampling; 2) identity-mapping shortcut, and projection shortcut at downsampling modules; 3) projection shortcut only. More types of shortcut connections were studied in [8] to determine the best type of shortcut connection for the performance. The experimental results in [8] showed that the identity-mapping shortcut connection is a much more appropriate choice than the following: 1) constant scaling shortcut; 2) projection shortcut; 3) gated shortcut. Since an identity-mapping shortcut connection purely passes through the gradient according to the identity-mapping and has fewer parameters, it has a lower possibility of overfitting than the other types of shortcut connections to ensure improved generalization ability.

In the case of our PyramidNet, the identity-mapping shortcut cannot be used since the feature map dimension differs among individual residual units. Therefore, only a zero-padded shortcut or projection shortcut can be used for all the residual units. However, as discussed in [8], a projection shortcut can hamper information propagation and lead to optimization problems, especially for very deep networks. On the other hand, we found that the zero-padded shortcut does not lead to the overfitting problem since no additional parameters exist, and surprisingly, it shows significant generalization ability compared to other shortcuts.

We now examine the effect of the zero-padded identity-mapping shortcut on the k -th residual unit in the n -th group with the reshaped vector \mathbf{x}_k^l of the l -th feature map:

$$\mathbf{x}_k^l = \begin{cases} \mathbf{F}_{(k,l)}(\mathbf{x}_{k-1}^l) + \mathbf{x}_{k-1}^l, & \text{if } 1 \leq l \leq D_{n,k-1} \\ \mathbf{F}_{(k,l)}(\mathbf{x}_{k-1}^l), & \text{if } D_{n,k-1} \leq l \leq D_{n,k} \end{cases} \quad (4)$$

where $D_{n,k}$ are the pre-defined channel dimensions of the k -th residual unit. From eq.(4), zero-padded elements of the identity-mapping shortcut for dimension increasing let \mathbf{x}_k^l contain the outputs of both residual networks and plain networks. Therefore, we could conjecture that each zero-padded identity-mapping shortcut can give the concatenations of the residual network and plain network as shown in Figure 5. Furthermore, our PyramidNet increases the channel dimension at every residual unit, and this effect increases markedly. Figure 4 supports the conclusion that the test error of the PyramidNet does not oscillate as much as that of the pre-activation ResNet.

3.3. A New Building Block

To maximize the capability of the network, it is natural to ask the following question: **“How does a good**

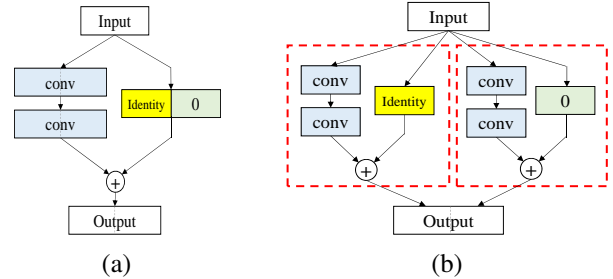


Figure 5. Structure of residual unit (a) with zero-padded shortcut, (b) unraveled view of (a) showing that the zero-padded identity-mapping shortcut constitutes a concatenation of a residual network with a skip connection and a plain network.

building block need to be stacked for improved performance?” The first type of building blocks were proposed in the original paper on ResNets [6], and another type of building block was subsequently proposed in the paper on pre-activation ResNets [8], to answer the question. Moreover, pre-activation ResNets tried to solve the backward gradient flowing problem [8] by redesigning residual modules and proved to be a successful trial. However, although the pre-activation residual unit was found experimentally, the possibility that there exists architecture capable of more optimal performance continues to prevail. We next attempt to answer the question from two points of view by considering Rectified Linear Units (ReLUs) [20] and Batch Normalization (BN) [11] layers.

3.3.1 ReLUs in a Building Block

Including ReLUs [20] in the building blocks of residual units is essential for nonlinearity, but we found empirically that the location and the number of ReLUs may degrade the performance. This could be discussed for original ResNets [6] for which it was shown that the performance increases as the model becomes deeper, but if the depth exceeds 1,000 layers, overfitting still occurs and the result is less accurate than for shallower ResNets.

First, we note that using ReLUs after the addition of residual units adversely affects the performance:

$$\mathbf{x}_k^l = ReLU(\mathbf{F}_{(k,l)}(\mathbf{x}_{k-1}^l) + \mathbf{x}_{k-1}^l), \quad (5)$$

where the ReLUs seem to have the function of filtering non-negative elements. Gross and Wilber [5] found that simply removing ReLUs from the original ResNet [6] after each addition leads to performance improvement by a small margin. This could be understood by considering that, after addition, ReLUs provide non-negative input to the subsequent residual units, and therefore the convolution layers only take responsibility for producing negative output before addition, which decreases the overall capability of the

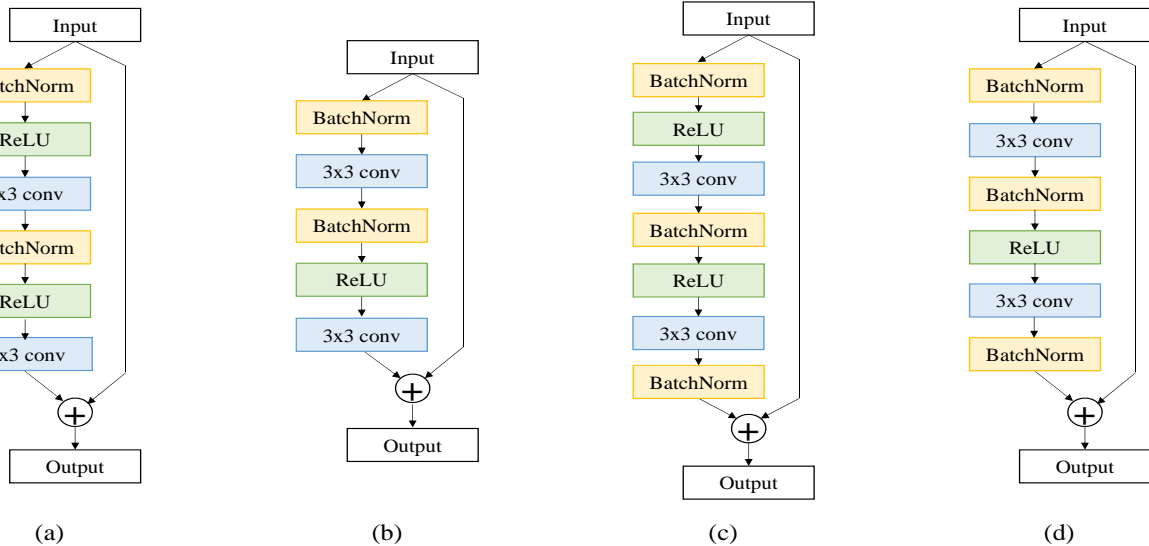


Figure 6. Various types of residual units. “BatchNorm” denotes the batch normalization layer. (a) original pre-activation ResNet [8], (b) single-ReLU pre-activation ResNet, (c) pre-activation ResNet with Batch Normalization (BN) after convolution layer, and (d) single-ReLU pre-activation ResNet with BN after convolution.

network architecture. The pre-activation ResNets proposed by He *et al.* [8] also overcame this issue with pre-activated residual units that traverse the BN layers and ReLUs before instead of after the convolution layers:

$$\mathbf{x}_k^l = \mathbf{F}_{(k,l)}(\mathbf{x}_{k-1}^l) + \mathbf{x}_{k-1}^l, \quad (6)$$

where ReLUs are removed after addition to create an identity path. Consequently, the overall performance has increased by a large margin without overfitting even at depths exceeding 1,000 layers. Furthermore, Shen *et al.* [24] proposed a weighted residual network architecture, which locates a ReLU inside a residual unit instead of after addition to create an identity path, and showed that this structure also does not overfit even at depths of more than 1,000 layers.

Second, we found that the use of a large number of ReLUs in the blocks of each residual unit may affect the performance negatively. The use of a single ReLU in the blocks of each residual unit, as shown in Figure 6 (b) and (d), was found to enhance the performance more than the corresponding two ReLUs in the blocks shown in Figure 6 (a) and (c). Experimentally, we found that removal of the first ReLU in the stack is preferable and that the other ReLU should remain to ensure nonlinearity. Removal of the second ReLU changes the blocks to *BN-ReLU-conv-BN-conv*, and it is clear that, in these blocks, the convolutional layers are successively located without ReLUs to weaken their representation powers of each other. However, when we remove the first ReLU, the blocks are changed to *BN-conv-BN-ReLU-conv*, in which case the two convolution layers are separated by the second ReLU, thereby guaranteeing

Case	CIFAR-10	CIFAR-100
Pre-activation ResNet [6]	5.15%	24.40%
Single-ReLU	4.81%	23.43%
BN after conv	4.96%	23.89%
BN after conv and single-ReLU	4.62%	23.31%

Table 2. Performance comparison for several combinations of ReLUs and BN layers. Top-1 error on CIFAR datasets using our pyramidal networks with different residual architectures.

nonlinearity. The results in Table 2 confirm that the use of a single ReLU, achieved by removing the first ReLU as in (c) and (d) in Figure 6 enhances the performance. Consequently, provided that an appropriate number of ReLUs are used to guarantee the nonlinearity of the feature space manifold, the remaining ReLUs could be removed to improve network performance.

3.3.2 BN Layers in a Building Block

The main role of a BN layer is to normalize the activations for fast convergence even with performance improvement. The experimental results of the four structures provided in Table 2 show that the BN layer can be used to maximize the capability of a single residual unit. A BN layer conducts affine transformation with the following equation:

$$\mathbf{y} = \gamma \mathbf{x} + \beta, \quad (7)$$

where γ and β are learned for every activation in feature maps. We experimentally found that the learned γ and β

could closely approximate 0. This implies that if the learned γ and β are both close to 0 then the corresponding activation is considered not to be useful. Weighted ResNets [24], in which the learnable weights occur at the end of their building blocks, are also similarly learned to determine whether the corresponding residual unit is useful. Thus, BN layers at the end of each residual unit are a generalized version including [24] to enable decisions to be made as to whether each residual unit is helpful. Therefore, the degrees of freedom obtained by involving γ and β from the BN layers could improve the capability of the network architecture. The results in Table 2 support that, addition of a BN layer at the end of each building block, as in type (c) and (d) in Figure 6, improves the performance. Note that the aforementioned single-ReLU network is also improved by adding a BN layer after convolution.

4. Experimental results

We evaluate and compare the performance of our algorithm with that of existing algorithms [6, 8, 18, 24, 33] on representative benchmark datasets: the CIFAR-10 and CIFAR-100 datasets [12]. Our results were mainly achieved by using multiplicative pyramidal residual networks, based on a normalized, single-ReLU pre-activation unit. Our code is built on the open source deep learning framework Torch [1].

4.1. Datasets

CIFAR-10. CIFAR-10 [12], which contains 32×32 -pixel color images, consists of 50,000 training images and 10,000 testing images in 10 classes. The standard data augmentation, horizontal flipping and translation by 4 pixels, are adopted in our experiments, following common practice [18].

CIFAR-100. CIFAR-100 [12] is a dataset which, similar to CIFAR-10, is also composed of 32×32 -pixel color images, and consists of 50,000 training images and 10,000 testing images, but includes 100 classes. The classes of CIFAR-100 are much more variable with an equal amount of data compared with CIFAR-10; thus, the CIFAR-100 dataset is more suitable to examine the regularization ability. In this case we also used standard data augmentation for training.

4.2. Training Settings

Our network is trained using backpropagation [15] by Stochastic Gradient Descent (SGD) with Nesterov momentum for 300 epochs on the CIFAR-10 and CIFAR-100 datasets. The initial learning rate is set to 0.5, decayed by a factor of 0.1 at 150 and 225 training epochs, respectively. The filter parameters are initialized by “msra” [7]. We use a weight decay of 0.0001, dampening to 0, and momentum of 0.9, with a batch size of 128.

4.3. Performance Evaluation

In our work, we mainly used the top-1 error rate for evaluating our model. This error rate is provided in Table 3 for our algorithm and the state-of-the-art algorithms. The experimental results show that our network has superior generalization ability, in terms of the number of parameters, showing the best results (smallest error) compared with other methods. For $\alpha = 16$, we found that our additive pyramidal residual network outperforms other methods such as ResNet and pre-activation Resnets with the same number of parameters.

The experimental results show that the performance of both additive and multiplicative PyramidNets are superior to other state-of-the-art methods. When the number of parameters is low, both additive and multiplicative PyramidNets show a similar performance, since these two models do not have significant structural differences. However, as the number of parameters increases, these models start to show a more marked difference in terms of the feature dimension structure. In case of the additive PyramidNets, since the feature dimension increases by linear decay, the feature dimensions of the upper layers tend to be larger and those of the lower layers smaller compared with the multiplicative PyramidNets. Simple visual illustrations of the two models are shown in Figure 2. Typically, researchers [6, 25] often use multiplicative scaling of the feature dimension for downsampling modules, which is implemented to improve the degree of freedom of the final layer (i.e., the classification descriptor) by increasing the feature dimension of the lower layers. Yet surprisingly, the experimental results show that the additive PyramidNets show improved performance. These results show that the upper layers, of which the feature map sizes are large, play a much more important role than the lower layers, indicating that increasing the model capacity of the upper layers would lead to a more optimal performance improvement than the lower layers.

We also note that, although the use of regularization methods such as dropout [28] or stochastic depth [10] could further improve the performance of our method, we selected not use these methods to ensure a fair comparison with other methods.

5. Conclusion

The novel deep network architecture in this paper involves a main idea increasing the feature map dimension gradually to construct so-called PyramidNet along with the concept of ResNets. We also studied a novel residual unit including a new building block of a residual unit with a zero-padded shortcut, which leads to significantly improved generalization ability. Our PyramidNets outperform all the previous state-of-the-art deep network architectures on the CIFAR-10 and CIFAR-100 datasets. Furthermore, the in-

Network	# params	Depth	CIFAR-10	CIFAR-100
NiN [18]	-	-	8.81%	35.68%
All-CNN [27]	-	-	7.25%	33.71%
DSN [17]	-	-	7.97%	34.57%
FitNet [21]	-	-	8.39%	35.04%
Highway [29]	-	-	7.72%	32.39%
Fractional Max-pooling [4]	-	-	4.50%	27.62%
ELU [29]	-	-	6.55%	24.28%
ResNet [6]	1.7M	110	6.43%	25.16%
ResNet [6]	10.2M	1202	7.93%	27.82%
Pre-activation ResNet [8]	1.7M	164	5.46%	24.33%
Pre-activation ResNet [8]	10.2M	1001	4.62%	22.71%
Stochastic Depth [10]	1.7M	110	5.23%	24.58%
Stochastic Depth [10]	10.2M	1202	4.91%	-
FractalNet [14]	38.6M	21	4.60%	23.73%
SwapOut v2 (width \times 4) [26]	7.43M	32	4.76%	22.72%
Wide ResNet (width \times 4) [33]	8.7M	40	4.97%	22.89%
Wide ResNet (width \times 8) [33]	11.0M	16	4.81%	22.07%
Wide ResNet (width \times 10) [33]	36.5M	28	4.17%	20.50%
Weighted ResNet [24]	19.1M	1192	5.10%	-
DenseNet [9]	27.2M	100	3.74%	19.25%
PyramidNet (mul, $\alpha = 1.68$)	1.7M	110	4.62%	23.16%
PyramidNet (add, $\alpha = 16$)	1.7M	110	4.62%	23.31%
PyramidNet (mul, $\alpha = 2$)	3.8M	110	4.50%	20.94%
PyramidNet (add, $\alpha = 28$)	3.8M	110	4.27%	20.21%
PyramidNet (mul, $\alpha = 3$)	28.3M	110	4.06%	18.79%
PyramidNet (add, $\alpha = 90$)	28.3M	110	3.77%	18.29%

Table 3. Top-1 error rates on CIFAR-10 and CIFAR-100 datasets. α denotes the widening factor; “add” and “mul” denote the results obtained with additive and multiplicative pyramidal networks, respectively.

sights in this paper could be utilized to any network architectures to improve their capability for better performance. For the future work, the way to construct the best network architecture, which is chosen by the optimized parameters including feature map dimension could be remained.

References

- [1] R. Collobert, K. Kavukcuoglu, and C. Farabet. Torch7: A matlab-like environment for machine learning. In *BigLearn, NIPS Workshop*, 2011. 7
- [2] J. Donahue, Y. Jia, O. Vinyals, J. Hoffman, N. Zhang, E. Tzeng, and T. Darrell. Decaf: A deep convolutional activation feature for generic visual recognition. In *ICML*, 2014. 1
- [3] R. Girshick, J. Donahue, T. Darrell, and J. Malik. Rich feature hierarchies for accurate object detection and semantic segmentation. In *CVPR*, 2014. 1
- [4] B. Graham. Fractional max-pooling. *arXiv preprint arXiv:1412.6071*, 2014. 8
- [5] S. Gross and M. Wilber. Training and investigating residual nets. 2016. <http://torch.ch/blog/2016/02/04/resnets.html>. 5
- [6] K. He, X. Zhang, S. Ren, and J. Sun. Deep residual learning for image recognition. In *CVPR*, 2015. 1, 2, 3, 4, 5, 6, 7, 8
- [7] K. He, X. Zhang, S. Ren, and J. Sun. Delving deep into rectifiers: Surpassing human-level performance on imagenet classification. In *ICCV*, 2015. 7
- [8] K. He, X. Zhang, S. Ren, and J. Sun. Identity mappings in deep residual networks. *arXiv preprint arXiv:1603.05027*, 2016. 1, 2, 3, 4, 5, 6, 7, 8
- [9] G. Huang, Z. Liu, and K. Q. Weinberger. Densely connected convolutional networks. *arXiv preprint arXiv:1608.06993*, 2016. 8
- [10] G. Huang, Y. Sun, Z. Liu, D. Sedra, and K. Weinberger. Deep networks with stochastic depth. *arXiv preprint arXiv:1603.09382*, 2016. 4, 7, 8
- [11] S. Ioffe and C. Szegedy. Batch normalization: Accelerating deep network training by reducing internal covariate shift. In *ICML*, 2015. 5
- [12] A. Krizhevsky. Learning multiple layers of features from tiny images. In *Tech Report*, 2009. 2, 7
- [13] A. Krizhevsky, I. Sutskever, and G. E. Hinton. ImageNet Classification with Deep Convolutional Neural Networks. In *NIPS*, 2012. 1, 2

- [14] G. Larsson, M. Maire, and G. Shakhnarovich. Fractalnet: Ultra-deep neural networks without residuals. *arXiv preprint arXiv:1605.07648*, 2016. 8
- [15] Y. LeCun, B. Boser, J. S. Denker, D. Henderson, R. E. Howard, W. Hubbard, and L. D. Jackel. Backpropagation applied to handwritten zip code recognition. *Neural computation*, 1(4):541–551, 1989. 7
- [16] Y. LeCun, L. Bottou, Y. Bengio, and P. Haffner. Gradient-based learning applied to document recognition. *Proceedings of the IEEE*, 86(11):2278–2324, 1998. 1
- [17] C.-Y. Lee, S. Xie, P. Gallagher, Z. Zhang, and Z. Tu. Deeply-supervised nets. In *AISTATS*, 2015. 8
- [18] M. Lin, Q. Chen, and S. Yan. Network in network. In *ICLR*, 2014. 7, 8
- [19] J. Long, E. Shelhamer, and T. Darrell. Fully convolutional networks for semantic segmentation. In *CVPR*, 2015. 1
- [20] V. Nair and G. E. Hinton. Rectified linear units improve restricted boltzmann machines. In *ICML*, 2010. 5
- [21] A. Romero, N. Ballas, S. E. Kahou, A. Chassang, C. Gatta, and Y. Bengio. Fitnets: Hints for thin deep nets. *arXiv preprint arXiv:1412.6550*, 2014. 8
- [22] O. Russakovsky, J. Deng, H. Su, J. Krause, S. Satheesh, S. Ma, Z. Huang, A. Karpathy, A. Khosla, M. Bernstein, A. C. Berg, and L. Fei-Fei. ImageNet Large Scale Visual Recognition Challenge. *International Journal of Computer Vision (IJCV)*, 115(3):211–252, 2015. 1
- [23] P. Sermanet, D. Eigen, X. Zhang, M. Mathieu, R. Fergus, and Y. LeCun. Overfeat: Integrated recognition, localization and detection using convolutional networks. *arXiv preprint arXiv:1312.6229*, 2013. 1
- [24] F. Shen and G. Zeng. Weighted residuals for very deep networks. *arXiv preprint arXiv:1605.08831*, 2016. 6, 7, 8
- [25] K. Simonyan and A. Zisserman. Very deep convolutional networks for large-scale image recognition. *arXiv preprint arXiv:1409.1556*, 2014. 1, 2, 3, 4, 7
- [26] S. Singh, D. Hoiem, and D. Forsyth. Swapout: Learning an ensemble of deep architectures. *arXiv preprint arXiv:1605.06465*, 2016. 8
- [27] J. T. Springenberg, A. Dosovitskiy, T. Brox, and M. Riedmiller. Striving for simplicity: The all convolutional net. In *ICLR Workshop*, 2015. 8
- [28] N. Srivastava, G. Hinton, A. Krizhevsky, I. Sutskever, and R. Salakhutdinov. Dropout: A simple way to prevent neural networks from overfitting. *Journal of Machine Learning Research*, 15:1929–1958, 2014. 7
- [29] R. K. Srivastava, K. Greff, and J. Schmidhuber. Training very deep networks. In *NIPS*, 2015. 1, 8
- [30] C. Szegedy, S. Ioffe, and V. Vanhoucke. Inception-v4, inception-resnet and the impact of residual connections on learning. *arXiv preprint arXiv:1602.07261*, 2016. 1
- [31] C. Szegedy, W. Liu, Y. Jia, P. Sermanet, S. Reed, D. Anguelov, D. Erhan, V. Vanhoucke, and A. Rabinovich. Going deeper with convolutions. In *CVPR*, 2015. 1, 2
- [32] A. Veit, M. Wilber, and S. Belongie. Residual networks are exponential ensembles of relatively shallow networks. *arXiv preprint arXiv:1605.06431*, 2016. 1, 2, 4
- [33] S. Zagoruyko and N. Komodakis. Wide residual networks. *arXiv preprint arXiv:1605.07146*, 2016. 2, 7, 8
- [34] M. D. Zeiler and R. Fergus. Visualizing and understanding convolutional networks. In *ECCV*, 2014. 1, 2